P2.8   **Simulations of Polarimetric Radar Signals Based on Numerical Weather Prediction Model Output**

Lei Lei[1,3], Guifu Zhang[2,3], Boon Leng Cheong[2,3], Robert D. Palmer[2,3], Ming Xue[2,4]

[1]School of Electrical and Computer Engineering, University of Oklahoma, Norman, OK
[2]School of Meteorology, University of Oklahoma, Norman, OK
[3]Atmospheric Radar Research Center (ARRC), University of Oklahoma, Norman, OK
[4]Center for Analysis and Prediction of Storms (CAPS), University of Oklahoma, Norman, OK

1. INTRODUCTION

Weather radar signals can be generated using either the spectrum method or Monte Carlo simulations. Zrnić (1975) simulated the time series data with the spectrum method. In Capsoni and D'Amico (1998), radar signals were simulated by summing the scattered wave fields from all contributing particles whose positions were randomly generated with Monte Carlo simulations. Capsoni et al. (2001) extended the above work to generate polarimetric radar signals. However, because of the computational requirements of the Monte Carlo approach, the radar data were generated for only a single range gate in their studies and therefore many aspects of the scanning radar were not simulated.

Recently, Cheong et al. (2008) developed a time series weather radar simulator that is capable of generating realistic, three-dimensional, time series radar data over many range gates and azimuth angles. The simulator uses thousands of scatters moving with the wind field produced from a high-resolution Advanced Regional Prediction System (ARPS) model (Xue et al. 2000). A table lookup and four-dimensional linear interpolation approach were used to simulate time series data from atmospheric parameters.

In this work, polarimetric capability is added to the radar simulator of Cheong et al. (2008). Horizontal and vertical channel signals are simultaneously produced. Propagation effects of attenuation, differential attenuation and extra phase shift are included. To be more realistic, the model output for a mixed-phase microphysics is used and contributions from five types of hydrometeors, i.e.: rain, snow, hail, rain-snow mixture and rain-hail mixture are accounted for. Polarimetric radar parameters such as differential reflectivity, differential phase and copolar cross correlation coefficient are calculated from the model output. Simulated radar signals are generated, which are three dimensional, time series and polarimetric radar data over many range gates and azimuth angles. By comparing the model-derived moments with the time-series-estimated moments, it has been demonstrated the simulator performs properly.

2. POLARIMETRIC RADAR SIMULATOR

The basic theory of the radar simulator is Monte Carlo integration. Each sample of horizontal and vertical composite signal is a complex sum of the baseband signal from all individual scatterers, which can be expressed mathematically as follows:

$$V_{h,v} = \sum_{l=1}^{n} A_{h,v}^{(l)} \exp[-j\phi_{h,v}^{(l)}] + N_{h,v} \qquad (1)$$

$$A_{h,v}(x,y,z) = (\frac{1}{r^4} w_a w_r Z_{h,v})^{0.5} \qquad (2)$$

$$\phi_{h,v}^{(l)} = 2\int_{0}^{r_l} (k_0 + \Delta k_{h,v}) dr \qquad (3)$$

where n is the total number of scatterers within the radar resolution volume. $(.)^{(l)}$ indicates the index of the lth discrete scatterers. Subscripts h and v stands for horizontal or vertical polarization, respectively. $A_{h,v}^{(l)}$ represents the amplitude of the signal from l^{th} scatterer. $\phi_{h,v}^{(l)}$ represents the phase of the lth scatterer. $N_{h,v}$ represents the additive white Gaussian noise. $Z_{h,v}$ is the equivalent reflectivity factor of the individual scatterers. w_a and w_r are the angular weight function and range weight function, respectively. The extra wave number $\Delta k_{h,v}$ is added to the free-space propagation constant k_0 in order to obtain the total effective propagation constant of hydrometer-filled medium. r_l is the distance of the lth scatterer from radar, where r_l is changing with time. Time series wind from the APRS updates the location of the scatterers.

Horizontal and vertical channel of signals are produced by Eq.(1), where the difference between horizontal and vertical channel signals comes from the two parameters $Z_{h,v}$ and $\Delta k_{h,v}$. Their calculations are provided in next two subsections.

2.1 Reflectivity factors

Reflectivity at horizontal (Z_h) and vertical (Z_v) polarizations are obtained as integrations over the drop size distribution (DSD) function weighted by the scattering cross section depending on density, shape, and orientation. For rain, dry snow, dry hail, rain-snow mixture, and rain-hail

mixture, we have (Zhang et al. 2001) the following:

$$Z_{(h,x)} = \frac{4\lambda^4}{\pi^4 |K_w|^2} \int n(D)(A|f_a|^2 + B|f_b|^2 + 2C|f_a||f_b|)dD \quad (4)$$

and

$$Z_{(v,x)} = \frac{4\lambda^4}{\pi^4 |K_w|^2} \int n(D)(B|f_a|^2 + A|f_b|^2 + 2C|f_a||f_b|)dD \quad (5)$$

where

$$A = <\cos^4\theta> = \frac{1}{8}(3 + 4\cos 2\bar{\theta}e^{-2\sigma^2} + \cos 4\bar{\theta}e^{-8\sigma^2}) \quad (6)$$

$$B = <\sin^4\theta> = \frac{1}{8}(3 - 4\cos 2\bar{\theta}e^{-2\sigma^2} + \cos 4\bar{\theta}e^{-8\sigma^2}) \quad (7)$$

$$C = <\sin^2\theta\cos^2\theta> = \frac{1}{8}(1 - \cos 4\bar{\theta}e^{-8\sigma^2}) \quad (8)$$

and x stands for r(rain), rs(rain-snow mixture), ds(dry snow), rh(rain-hail mixture), or dh(dry hail). Here f_a and f_b are backscattering amplitudes for polarizations along the major and minor axes, respectively. $n(D)$ is DSD. $\bar{\theta}$ is the mean canting angle and σ is the standard deviation of the canting angle. (Jung et al. 2008) Their values are listed in the following Table.1.:

Table.1. Mean canting angle $\bar{\theta}$, and the standard deviation of the canting angle σ for rain, snow and hail.

	$\bar{\theta}$, degree	σ, degree
Rain	0	0
Snow	0	20
Hail	0	$60(1-cf_w)$

For the purpose of computational efficiency, the scattering amplitudes are parameterized as a set of power-law functions of the hydrometeors' size (Zhang et al. 2001; Jung et al. 2008). The parameterization results were based on the T-matrix calculation for raindrops and Rayleigh scattering approximation for oblate spheroids is applied to snow and hail particles. Hence, analytical expressions of the reflectivities are obtained as

$$Z_{h,x} = \frac{4\lambda^4 N_{0x}}{\pi^4 |K_w|^2} \Lambda_x^{-(2\beta_{xa}+1)}\Gamma(2\beta_{xa}+1)$$
$$\cdot (A\alpha_{xa}^2 + B\alpha_{xb}^2 + 2C\alpha_{xa}\alpha_{xb}) \quad (9)$$

and

$$Z_{v,x} = \frac{4\lambda^4 N_{0x}}{\pi^4 |K_w|^2} \Lambda_x^{-(2\beta_{xb}+1)}\Gamma(2\beta_{xb}+1)$$
$$\cdot (B\alpha_{xa}^2 + A\alpha_{xb}^2 + 2C\alpha_{xa}\alpha_{xb}) \quad (10)$$

In the above equations, default values for intercept parameter N_{ox} from the Lin et al.(1983) microphysics scheme used in the ARPS are assumed. x represents the species type, i.e., rain, hail, snow, rain-snow mixture or rain-hail mixture. The detailed description of the parameters can be found in Jung et al. (2008)

Once the reflectivity factors are known for each species, the total equivalent reflectivity factors are calculated by

$$Z_h = Z_{h,r} + Z_{h,rs} + Z_{h,ds} + Z_{h,rh} + Z_{h,dh} \quad (11)$$
$$Z_v = Z_{v,r} + Z_{v,rs} + Z_{v,ds} + Z_{v,rh} + Z_{v,dh} \quad (12)$$

These equivalent reflectivities are then used as input for the process of generating time series radar data. Parameterization methods can speed up computations is the emulator which is important for simulations for large domains. For better accuracy, directly integration of Eqs (4) and (5) is performed to calculate equivalent reflectivities. T-matrix calculation is computational complex but more accurate than parameterization method. These two methods are built as options in the simulator and can be chosen depending on the different purposes.

2.2 Propagation phase

For the phase part in Eq. (1), propagation constants k_h and k_v are given by

$$k_{h,v} = k_0 + \Delta k_{h,v}$$

with

$$\Delta k_{h,v} = \frac{180\lambda}{\pi} \int n(D)E\,\text{Re}(f_{a,b})dD$$

where, $E = <\cos 2\theta> = \cos 2\bar{\theta}e^{-2\sigma^2}$ \quad (13)

The parameterization of the five hydrometeor species is described as follows:

$$\Delta k_{h,v} = \frac{180\lambda}{\pi} N_{0x}E\alpha_{kx}\Lambda^{-(\beta_{kx}+1)}\Gamma(\beta_{kx}+1) \quad (14)$$

For rain, we assume

$$\text{Re}(f_a) = \alpha_{kra}D^{\beta_{kra}} \quad, \quad \text{Re}(f_b) = \alpha_{krb}D^{\beta_{krb}}$$
$$\alpha_{kra} = \alpha_{krb} = 3.88\times 10^{-4}$$

where, $\quad \beta_{kra} = 3.16$

$$\beta_{krb} = 2.97$$

For other species, we assume Rayleigh scattering. In this regime, scattering is isotropic, which means that the forward and backward scatterings are the same. It enables us to use backward scattering instead of forward scattering. The image part of $f_{a,b}$ is small compared to the real part. We can therefore use $|f_{a,b}|$ instead of $\text{Re}(f_{a,b})$ for other species. α_{kx} can be calculated directly using the same formula as that for calculating equivalent reflectivity. β_{kx} is equal to 3.

For parameterization method, Δk can be calculated from the ARPS' data using Eq.(14). Then, the data is projected to radar beam grid and stored in three dimensional manner, (in azimuth, elevation and range), where finer a mesh grid produces better accuracy in radar echoes. After that, for each scatterer Δk is integrated through the two way path from radar to scatterer to get the phase part in Eq. (3). Then, phase data is input into the process of generating time series radar data. For better accuracy, directly integration of Eq. (13) is used to calculate k. Similar to the

equivalent reflectivity, either the parameterization method or direct integration method can be chosen depending on purposes.

2.3 Correlation coefficient

The correlation coefficient is calculated as:

$$\rho_{hv} = \frac{|Z_{hv,r} + Z_{hv,s} + Z_{hv,h} + Z_{hv,rs} + Z_{hv,rh}|}{(Z_{h,r} + Z_{h,s} + Z_{h,h} + Z_{h,rs} + Z_{h,rh})^{0.5}} \tag{15}$$

$$\cdot \frac{1}{(Z_{v,r} + Z_{v,s} + Z_{v,h} + Z_{v,rs} + Z_{v,rh})^{0.5}}$$

where

$$Z_{hv,x} = \frac{4\lambda^4}{\pi^4 |K_w|^2} \int_0^{D_{max,x}} [C(|f_{a,x}(\pi)|^2 + |f_{b,x}(\pi)|^2) \tag{16}$$

$$+2F|f_{a,x}(\pi)||f_{b,x}(\pi)|\rho_{0,x}]n(D)dD$$

$$F = <\cos^4\theta + \sin^4\theta> = \frac{1}{8}(3 + \cos 4\bar{\theta}e^{-8\sigma^2}) \tag{17}$$

3. RADAR SIGNAL GENERATION AND PARAMETER ESTIMATION

The model output that is used to test our radar simulator was produced by the ARPS model (Xue at al. 2000, 2001). The prognostic state variables include the three wind components, potential temperature, pressure, turbulent kinetic energy, mixing ratios for water vapor, rain water, cloud water, cloud ice, snow and hail. In this dataset, there is a super-cell storm simulated with 50-m horizontal

resolution in $64\times64\times16$ km^3 domain. For the computation being manageable for the radar simulator, we choose a smaller subdomain from the simulations as shown in Fig.1.
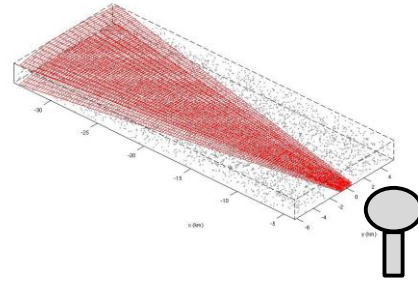

FIG.1. Configuration of simulation domain and radar location.

To generate time series data, the radar parameters used are listed as follows:

Average number of scatterers per volume: 30
Frequency: 2.7×10^9 Hz
Dish radar at (0,0,0)
PRT: 1.0×10^{-3} s
τ: 1.57×10^{-6} s
azimuth beam width: 0.95 degree
elevation beam width: 0.95 degree
elevation: 0.5 degree
azimuth extend: [-100.0 ... -81.0] degree
azimuth step: 1.0 degree
minimum range: 4000.0 m
gate width: 235 m
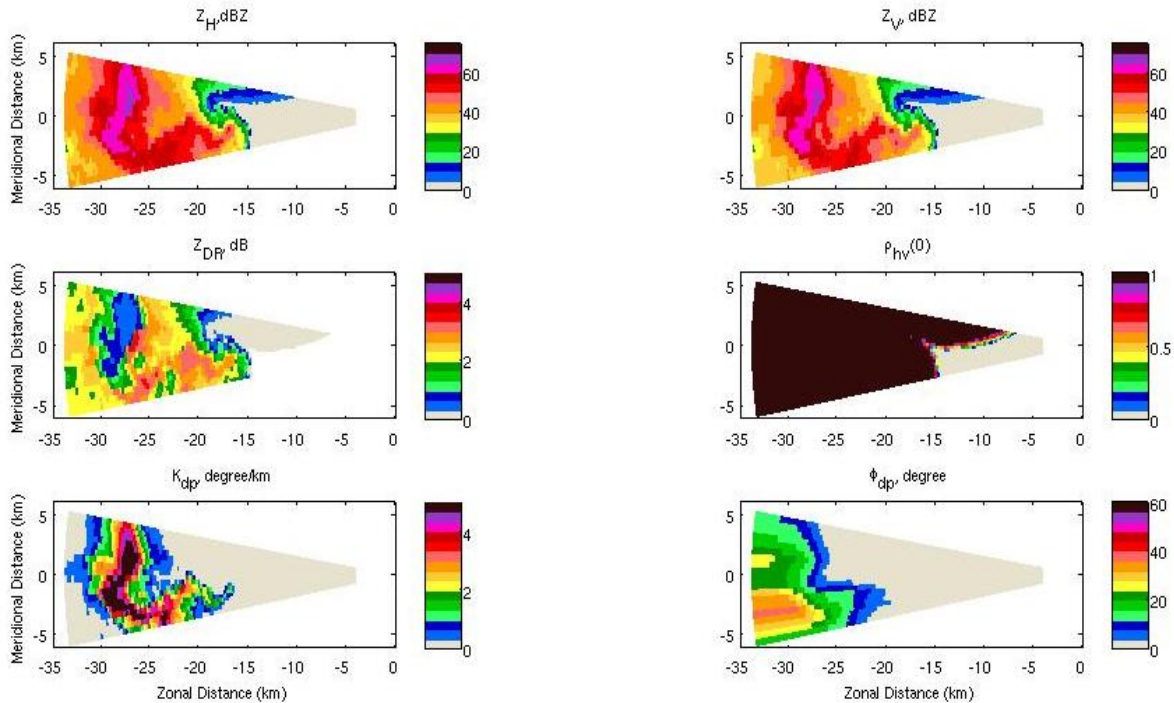number of gates: 128
number of pulses: 32

FIG.2. Example parameters that can be derived from the ARPS data. The ARPS grid is projected to radar beam.

Polarimetric radar parameters are calculated from the ARPS' variables including water mixing ratio, hail mixing ratio, snow mixing ratio are shown in Fig.2. This is used to verify our radar simulator result.

$$\hat{K}_{DP}(r_0) = \frac{\sum[\phi_{DP}(r_i) - \bar{\phi}_{DP}(r_i)](r_i - r_0)}{2\sum_i (r_i - r_0)^2} , \qquad (18)$$

After the time series data are generated and simulated white noise is added, the polarimetric radar parameters are estimated by

$$\hat{Z}_{h,v} = \frac{1}{M}\sum_{m=1}^{M}|V_{h,v}(m)|^2 ,$$

$$\hat{Z}_{DR} = 10\log10(\frac{\hat{Z}_h}{\hat{Z}_v}) ,$$

$$\hat{R}_{h,v} = \frac{1}{M}\sum_{m=1}^{M-|n|}V_{h,v}(m)^*V_{h,v}(m+n),$$

$$\hat{R}_{hv} = \frac{1}{M}\sum_{m=1}^{M-|n|}V_{h}(m)^*V_{v}(m+n),$$

$$\hat{\rho}_{hv} = \frac{|\hat{R}_{hv}(0)|}{\sqrt{\hat{Z}_h\hat{Z}_v}} ,$$

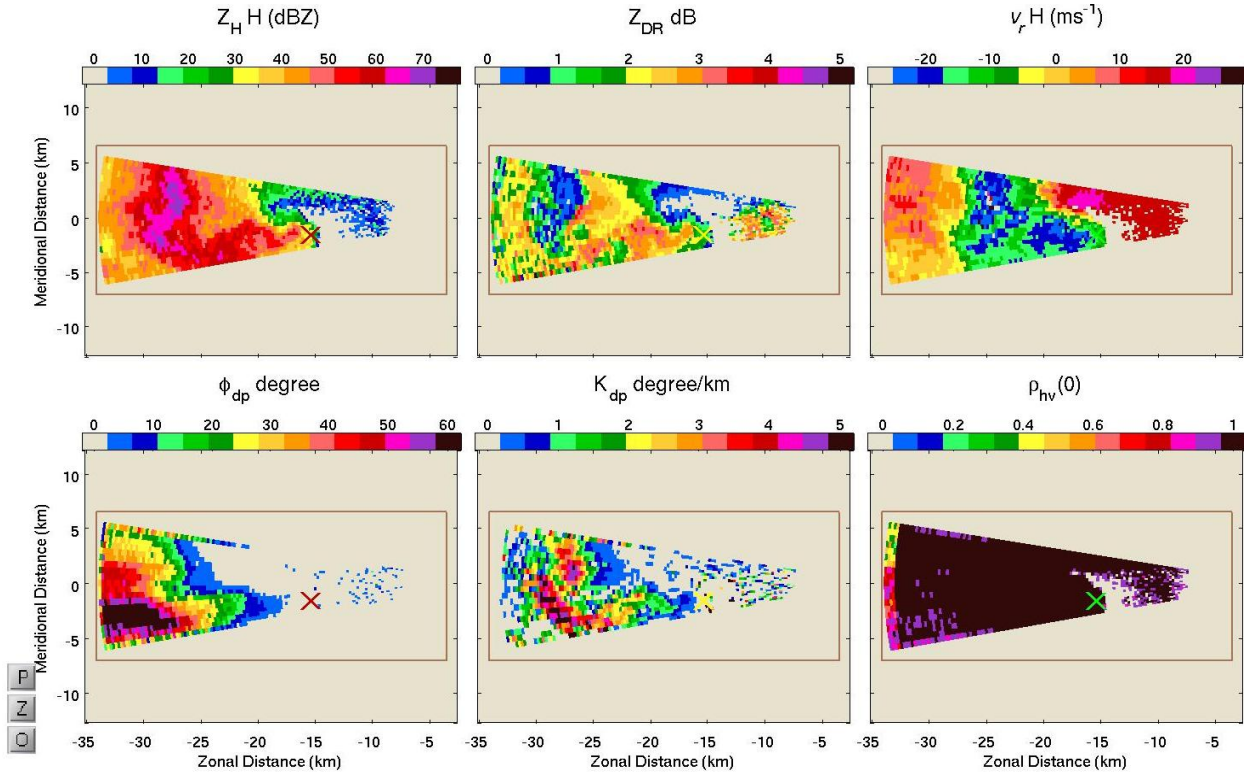$$\phi_{DP} = \frac{1}{2}\arg(R_h^*(0)R_v(0)) ,$$

FIG.3. Polarimetric radar parameters estimated from the radar simulator generated time series data with noise. SNR=60dB
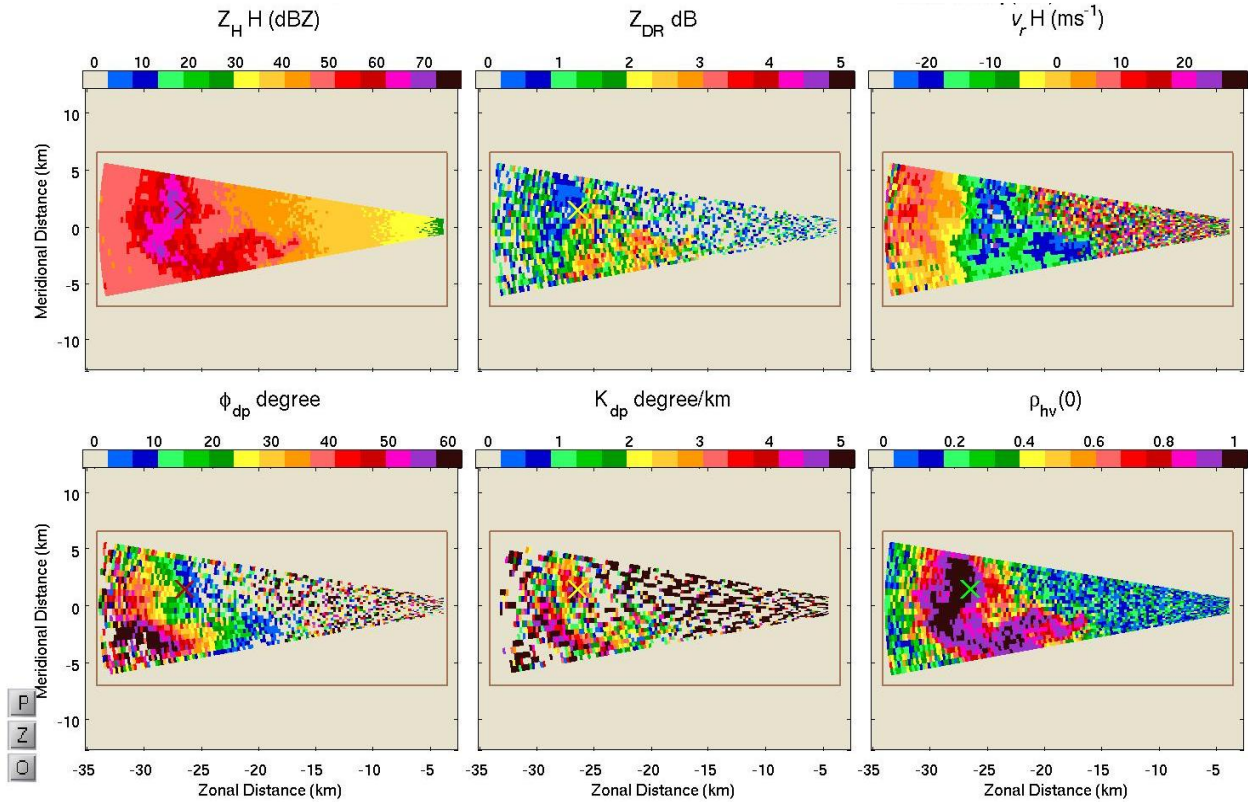
FIG.4. Polarimetric radar parameters estimated from the radar simulator generated time series data with noise. SNR=10dB

The polarimetric radar parameters estimated from the radar simulator-generated time series data are show in Fig.3. and Fig.4.for signal to noise ratios(SNR) of 60dB and 10dB, respectively. It can be seen between the ranges of 25km to 30km where large amount of hail exists that there is a region of Z_{DR} decreases. When the signal-to-noise ratio is 10dB(Fig.4), while the main reflectivity and ρ_{hv} signatures associated with precipitation core are preserved. Polarimetric parameters of Z_{DR} and K_{DP} are degraded due to the added noise and sampling error. With the increase of white noise, ρ_{hv} decreases and meaningful pattern only shows in the heaviest precipitation regions. This shows that it is important to have a high SNR to produce high quality polarimetric radar data. Advanced signal processing could be used to improve the polarimetric signals.

Comparison between Fig.2 and Fig.3. shows that the radar simulator results are consistent with the model output. In general, the estimated polarimetric radar parameters are consistent with our expectations and observations of real storms.

4. SUMMARY

We reported on a polarimetric radar simulator that can take different types of numerical model output and, generate physically based time-series radar data in a three-dimensional space for H and V channels. The estimated moment data carry the polarimetric radar signature. By comparing the model-derived moments with the time-series-estimated moments, it has been demonstrated the simulator performs properly. The simulator can be used to develop and test advanced signal processing algorithms. The results shown were for S-band, but, all the input parameters are tunable by the user, including radar wavelength.

References:

Cheong, B.L., Palmer, R. D., and Xue, M., 2008: A time series weather radar simulator based on high-resolution atmospheric models. *J. Atmos. Oceanic Technol.*,**25**, 230-243.

Capsoni, C., and M. D'Amico, 1998: A physically based radar simulator. *J. Atmos. Oceanic Technol.*, **15**, 593-598.

Capsoni, C., and M. D'Amico, and R. Nebuloni, 2001: A multiparameter polarimetric radar simulator. *J. Atmos. Oceanic Technol.*, **18**, 1799-1809.

Doviak, R.J., and D. S. Zrnić, 1993: Doppler Radar and Weather Observations. 2nd ed. Academic Press, pp 154-156.

Jung, Y., Zhang, G., and Xue, M., 2008: Assimilation of

simulated polarimetric radar data for a convective storm using the ensemble Kalman filter. Part I: Observation operators for reflectivity and polarimetric variables. *Mon. Wea. Rev.,***136**(6), 2228–2245, 2008

Lin, Y.-L., Farley R. D., and Orville H. D., 1983: Bulk parameterization of the snow field in a cloud model. *J. Climate Appl. Meteor.*, **22,** 1065-1092.

Oguchi T., 1983:Electromagnetic Wave Propagation and Scattering in Rain and Other Hydrometeors. *IEEE*, **71**, No.9

Xue, M., K.K. Droegemeier, and V. Wong, 2000: The Advanced Regional Prediction System (ARPS)-----A multiscalenonhydrostatic atmospheric simulation and prediction tool. Part I: Model dynamics and verification. *Meteor. Atmos. Phys.*, **75**, 161-193.

Xue, M., and Coauthors, 2001: The Advanced Regional Prediction System(ARPS)-----A multiscalenonhydrostatic simulation and prediction tool. Part II: Model physics and applications. *Meteor. Atmos. Phys.*, **76**,143-165.

Zhang, G., J. Vivekanandan, and E. Brandes, 2001: A method for estimating rain rate and drop size distribution from polarimetric radar measurements. *IEEE Trans. Geosci. Remote Sens.*, **39**, 830-841.

Zrnić, D. S., 1975: Simulation of weatherlike Doppler spectra and signals. *J. Appl. Meteor.*, **14**, 619-620.